Available online at www.elixirpublishers.com (Elixir International Journal)

Chemical Physics Letters

Elixir Chem. Phys. Letters 71 (2014) 24862-24868

ISSN: 2229-712X

Density functional theory study of Fourier transform Infrared and Raman spectra of 2-amino-5-nitropyrimidine

M.K.Subramanian* and D.Brundha

Post Graduate and Research Department of Physics, Thiruvalluvar Government Arts College, Rasipuram, India.

ARTICLE INFO

Article history:
Received: 15 April 2014;
Received in revised form:
6 June 2014;
Accepted: 11 June 2014;

Keywords
Density Functional Theory,
FT-Raman,
FT-IR,
HOMO,
LUMO,
First-order Hyperpolarizability.

ABSTRACT

The vibrational spectral analysis was carried out by using Raman and infrared spectroscopy in the range 4000–400 cm^{-1} and 4000–100 cm^{-1} respectively, for 2-amino-5-nitropyrimidine (2A5NP) molecule. The molecular structure, fundamental vibrational frequencies and intensity of the vibrational bands are interpreted with the aid of structure optimizations and normal coordinate force field calculations based on density functional theory (DFT) method and different basis sets combination. The complete vibrational assignments of wavenumbers were made on the basis of potential energy distribution (PED). The scaled B3LYP/6-311++G results show the best agreement with the experimental values over the other methods. The calculated HOMO and LUMO energies shows that charge transfer within the molecule. The results of the calculations were applied to simulate spectra of the title compound, which show excellent agreement with observed spectra. Electronic excitation energies, oscillator strength and nature of the respective excited states were calculated by the closed-shell singlet calculation method were also calculated for the molecule.

Introduction

The Pyrimidine ring system has wide occurrence in nature as substituted and ring fused compounds and derivatives, including the nucleotides, thiamine (vitaminB1) and alloxan. It is also found in many synthetic compounds such as barbiturates and the HIV drug, zidovudine. Although Pyrimidine derivatives such as uric acid and alloxan were known in the early 19th century, a laboratory synthesis of a Pyrimidine was not carried out until 1879, when Grimaux reported the preparation of barbituric acid from Ivy urea and malonic acid in the presence of phosphorus oxychloride. The systematic study of Pyrimidines began in 1884 with Pinner, who synthesized derivatives by condensing ethyl acetoacetate with amidines. Pinner first proposed the name "Pyrimidin" in 1885.

Pyrimidine and its derivatives are known for their biological and pharmaceutical importance. The properties are determined by their hydrogen and π bonding systems. They belong to the family of nucleic acids. Nucleic acids are of great interest, since, they control the manufacture of proteins and the functions of the cells in living organisms [1–3]. Due to low toxicity and wide ranging application derivatives of pyrimidines, we have undertaken a thorough vibrational analysis of 2-amino-5-nitropyrimidine and density functional theory (DFT) calculations. The results of the TED calculations are also useful for understanding the delocalization of electrons involved in this compound.

The aim of this work is to check the performance of B3LYP density functional force field for simulation of IR and Raman spectra of the title compound 2-amino-5-nitropyrimidine (2A5NP) with the use of standard 6-31G* and 6-311+G** basis sets (referred to as small and large basis set, respectively). The simulated and observed spectra were analysed in detail. Unambiguous vibrational assignment of all the fundamentals was made using the total energy distribution (TED). Density functional theory calculations were performed for the title compound to evaluate the first order hyperpolarizability value. The calculated HOMO and LUMO energies shows that charge transfer occur within the molecule. Electronic excitation energies, oscillator strength and nature of the respective excited states were calculated by the closed-shell singlet calculation method were also calculated for the molecule.

Experimental details

The sample of 2A5NP was obtained from Lancaster chemical company, UK, and used, as such for the spectral measurements. The FT-Raman spectra was recorded on a computer interfaced BRUKER IFS model interferometer equipped with FRA 106 FT-Raman accessories. The spectrumwas recorded in the region 3500–100 cm^{-1} with Nd:YA Glaser operating at 200mW power continuously with 1064 nm excitation. The room temperature mid infrared spectrum of the title compound was measured in the region 4000–400 cm^{-1} at a resolution of ±1 cm^{-1} using Perkin-Elmer RX1 Fourier transform spectrometer equipped with LiTaO3 detector, a KBr beam splitter and He–Ne Laser source. Boxcar apodization was used for the 250 averaged interferrograms, collected for the sample.

Computational details

The calculation of the vibrational frequencies is essential and also useful for the vibrational assignments of the spectra. Quantum chemical calculations for 2A5NP was performed with the GAUSSIAN 03W program [4] using the Becke 3-Lee-Yang-Parr (B3LYP) functional [5,6] supplemented with the standard 6-311 + G** basis set (referred to as large basis set), for the Cartesian representation of the theoretical force constants have been computed at the fully optimized geometry by assuming *Cs* point group symmetry. Scaling of the force field was performed according to the SQM procedure [7,8] using selective (multiple) scaling in the natural internal coordinate representation [9]. Transformations of the force field and the subsequent normal coordinate analysis including the least squares refinement of the

---

Tele:
E-mail addresses: profdrmks@gmail.com

scaling factors, calculation of total energy distribution (TED) and IR and Raman intensities were done on a PC with the MOLVIB program (Version V7.0-G77) written by Sundius [10,11]. The TED elements provide a measure of each internal coordinates contribution to the normal coordinate. For the plots of simulated IR and Raman spectra, pure Lorentzian band shapes were used with a bandwidth (FWHH) of 10 cm^{-1}.

The prediction of Raman intensities was carried out by following the procedure outlined below. The Raman activities calculated by the GAUSSIAN 03W program and adjusted during scaling procedure with MOLVIB were converted to relative Raman intensities using the following relationship derived from the basic theory of Raman scattering [12-13].

$$I_i = \frac{f(\nu_o-\nu_i)^4 S_i}{\nu_i[1-\exp(-hc\nu_i/KT)]} \quad \text{--------------(1)}$$

Where υ_0 is the exciting frequency (in cm^{-1}), υ_i is the vibrational wavenumber of the i^{th} normal mode; h, c and k are fundamental constants, and f is a suitably chosen common normalization factor for all peak intensities.

Results and discussion

Molecular geometry

The global minimum energy obtained by the DFT structure optimization was presented in Table 1. The optimized geometrical parameters obtained by the large basis set calculation were presented in Table 2. The optimized molecular structure of 2A5NP was shown in Fig. 1.

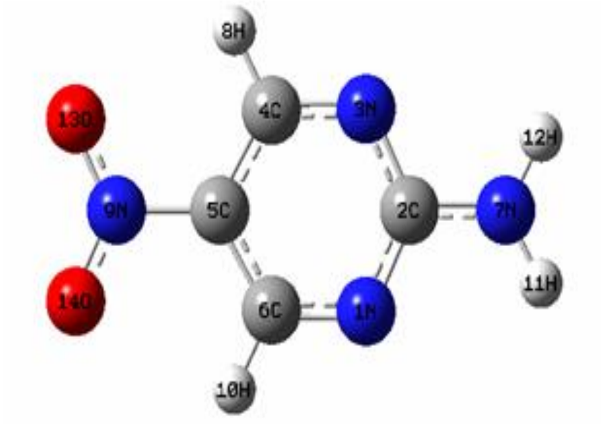

Fig. 1. The optimized molecular structure of 2A5NP

Analysis of vibrational spectra

The 36 normal modes of 2A5NP are distributed among the symmetry species as Γ_{3N-6}= 25 A' (in-plane) + 11 A″ (out-of-plane), and in agreement with C_s symmetry. All the vibrations were active both in Raman scattering and infrared absorption. In the Raman spectrum the in-plane vibrations (A') give rise to polarized bands while the out-of-plane ones (A″) to depolarized band.

Detailed description of vibrational modes can be given by means of normal coordinate analysis (NCA). For this purpose, the full set of 48 standard internal coordinates containing 12 redundancies were defined as given in Table 3. From these, a non-redundant set of local symmetry coordinates were constructed by suitable linear combinations of internal coordinates following the recommendations of Fogarasi et. al [14] are summarized in Table 4. The theoretically calculated DFT force fields were transformed in this later set of vibrational coordinates and used in all subsequent calculations.

The detailed vibrational assignments of fundamental modes of 2A5NP along with calculated IR, Raman intensities and normal mode descriptions (characterized by TED) were reported in Table 5. For visual comparison, the observed and simulated FT-IR and FT-Raman spectra of 2A5NP are produced in a common frequency scales in Fig. 2 & Fig. 3.

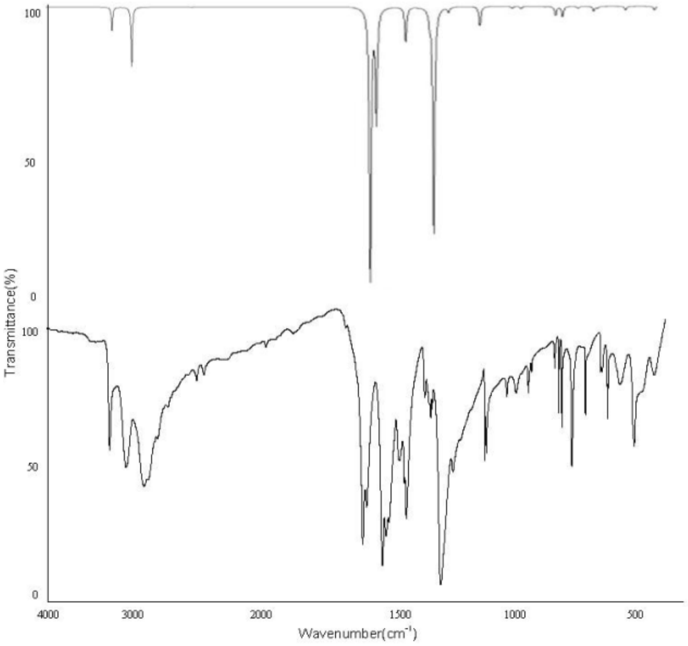

Fig. 2. FT-IR spectra of 2A5NP
(a)Observed (b) Calculated with B3LYP/6-311+G**

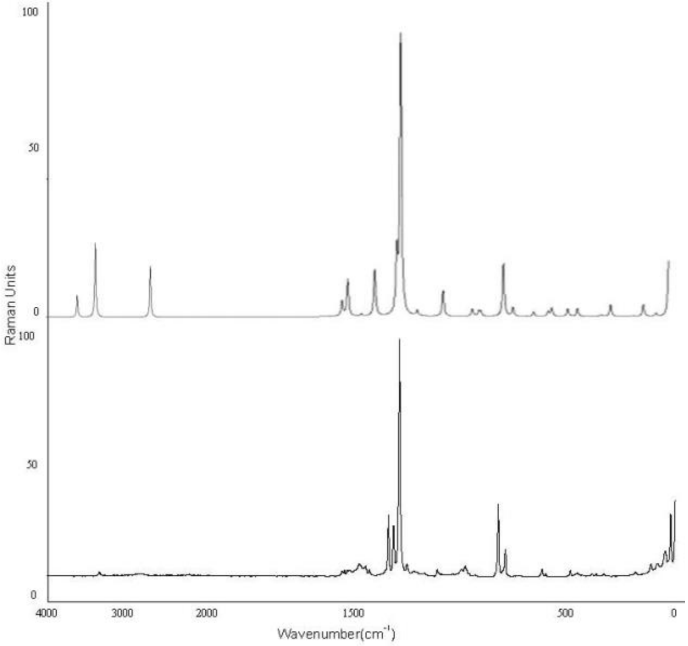

Fig. 3. FT-Raman spectra of 2A5NP
(a) Observed (b) Calculated with B3LYP/6-311+G**

Root mean square (RMS) values of frequencies were obtained in the study using the following expression,

$$\mathrm{RMS} = \sqrt{\frac{1}{n-1}\sum_{i}^{n}\left(\upsilon_i^{calc}-\upsilon_i^{exp}\right)^2}$$

The RMS error of the observed and calculated frequencies (unscaled / B3LYP/6-311+G**) of 2A5NP was found to be 115 cm^{-1}. This is quite obvious; since the frequencies calculated on the basis of quantum mechanical force fields usually differ appreciably from observed frequencies. This is partly due to the neglect of anharmonicity and partly due to the approximate nature of the quantum mechanical methods. In order to reduce the overall deviation between the unscaled and observed fundamental frequencies, scale factors were applied in the normal coordinate analysis and the subsequent least square fit refinement algorithm resulted into a very close agreement between the observed fundamentals and the scaled frequencies. Refinement of the scaling factors applied in this study achieved a weighted mean deviation of 7.8 cm^{-1} between the experimental and scaled frequencies of the title compound.

Table 1. Total energies of 2A5NP, calculated at DFT (B3LYP)/6-31G* and (B3LYP)/6-311+G level**

Method	Energies (Hartrees)
6-31G*	-524.1659524
6-311+G**	-524.1953770

C-H vibrations

Aromatic compounds commonly exhibit multiple weak bands in the region 3100–3000 cm^{-1} due to aromatic C-H stretching vibrations. The bands due to C-H in-plane bending vibration interact with C-C stretching vibrations, are observed as a number of bands in the region 1300–1000 cm^{-1}. The C-H out-of-plane bending vibrations occur in the region 900–667 cm^{-1} [15]. In this region the bands are not affected appreciably by the nature of the subsituents. In the present investigation, the IR bands identified at 3200–3230 cm^{-1} are assigned to C-H stretching vibration. The bands observed at 1415, 1414, 1396, 1330, 1327, 1195, 1190, 1187, 1049 and 1046 cm^{-1} were assigned to C-H inplane bending vibration. The C-H out of plane bending modes was assigned within characteristic region and were presented in Table 5.

C-C vibrations

The bands between 1480 and 1650 cm^{-1} are assigned to C–C stretching modes [16]. In the present study, the carbon stretching vibrations of the title compound have been observed at 1585, 1582, 1578, 1415, 1414 and 1410 cm^{-1} in the FT-IR and 1655, 1649 and 1647 cm^{-1} in FT-Raman spectrum. The in-plane and out-of-plane bending vibrations of C–C group were presented in Table 4.5. These assignments are in good agreement with literature [17].

C-N vibrations

The identification of C-N vibrations is a difficult task, since the mixing of vibrations is possible in this region. However, with the help of force field calculations, the C-N vibrations are identified and assigned in this study. The slight shift in wavenumber in due to the fact that force constants of the C-N bond increases due to resonance with the ring. Absorbances are also observed at 1640–1620 cm^{-1}, 1580–1520 cm^{-1}, 1000–960 cm^{-1} and 825–775 cm^{-1}. Accordingly the bands observed at 1673, 1655, 1649, 1647, 1585, 1582, 1578, 1525, 1520, 1516, 1190, 1187, 1049, 1046 and 1043 cm^{-1} have been assigned to C-N stretching modes and their corresponding TED modes are, respectively.

Amino group vibrations

The frequencies of amino group appear in the regions 3500–3300 cm^{-1} for N-H stretching, 1700–1600 cm^{-1} for scissoring and 1150–900 cm^{-1} for rocking deformations [18]. In the present study, the asymmetric and symmetric modes of NH_2 group were assigned at 3755, 3752, 3626, 3623 and 3621 cm^{-1} respectively. The band observed at 1677, 1674, 1673, 1655, 1649, 1647 cm^{-1} is assigned to NH_2 scissoring mode. The rocking, wagging deformation vibrations of NH_2 contribute to several normal modes in the low frequency region. The band observed at 1330, 1327, 1316, 1312, 1046, 1043 and 1034 cm^{-1} to NH_2 rocking vibration and the band observed at 415, 413 and 409 cm^{-1} is assigned to NH_2 wagging mode. The wagging and torsional modes of NH_2 were identified at 162 and 159 cm^{-1} respectively.

Nitro group vibrations

The NO_2 group is predominantly subject to the attractive interaction by the NH_2 group of the neighboring molecule due to intermolecular hydrogen bonding. Aromatic nitro compounds have strong absorptions due to asymmetric and symmetric stretching vibrations of the nitro group at 1570–1485 and 1370–1320 cm^{-1}. Usually, the symmetric vibration is stronger than antisymmetric one in the Raman spectra and the contrary holds in infrared [19,20]. This could be due to the electron withdrawing substituent adjacent to the nitro group tend to increase the frequency of asymmetric vibration and decrease that of the symmetric vibration. Thus, the band due to the asymmetric stretching vibration for nitro groups forced out of plane of the ring by bulky substituent was found at 1585, 1582 and 1578 cm^{-1} with strong intensity in the compound 2A5NP. The symmetric stretching vibrations of this group were found intense at 1396, 1395 and 1385 cm^{-1}.

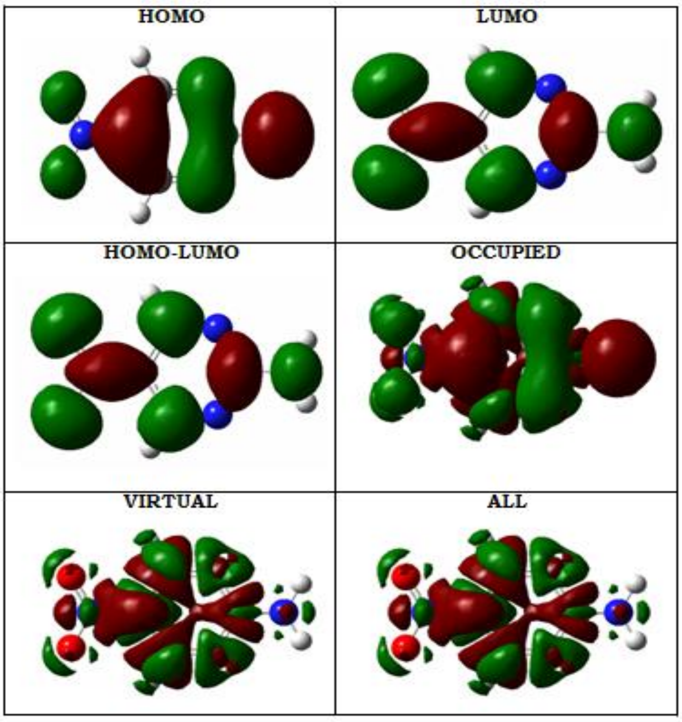

Fig. 4. Representation of the orbital involved in the electronic transition for (a) HOMO (b) LUMO (c) HOMO, LUMO (d) Occupied (e) Virtual (f) All

Hyperpolarizability calculations

The first-order hyperpolarizibility (β_{ijk}) of the novel molecular system of 2A5NP is calculated using 3-21 G (d,p) basis set based on finite field approach. Hyperpolarizibility is a third rank tensor that can be described by a 3 x 3 x 3 matrix. It strongly depends on the method and basis set used. The 27 components of 3D matrix can be reduced to 10 components due to Kleinman [21] symmetry. The calculated first-order hyperpolarizability (β_{total}) of 2A5NP is $4.2557x10^{-30}$ esu, which is nearly 22 times greater than that of urea (0.1947×10^{-30} esu). The calculated dipole moment (μ) and first-order hyperpolarizibility (β) are shown in Table 6. The theoretical calculation seems to be more helpful in determination of particular components of β tensor than in establishing the real values of β. Domination of particular components indicates on a substantial delocalization of charges in those directions. It is noticed that in β_{xyy} (which is the principal dipole moment axis and it is parallel to the charge transfer axis) direction, the biggest values of hyperpolarizability are noticed and subsequently delocalization of electron cloud is more in that direction. The higher dipole moment values are associated, in general, with even larger projection of β_{total} quantities.

Table 2. Optimized geometrical parameters of 2A5NP obtained by B3LYP/ 6–311+G density functional calculations**

Bond length	Value(Å)	Bond angle	Value(Å)	Dihedral angle	Value(Å)
C2-N1	1.30144	N3-C2-N1	120.00020	C4-N3-C2-N1	0.00000
N3-C2	1.30136	C4-N3-C2	120.00100	C5-C4-N3-C2	0.00000
C4-N3	1.30140	C5-C4-N3	123.32972	C6-N1-C2-N3	0.00000
C5-C4	1.26124	C6-C1-N2	119.99879	N7-C2-N1-C6	-179.42801
C6-N1	1.30140	N7-C2-N1	119.99756	H8-C4-N3-C2	179.46042
N7-C2	1.44605	H8-C4-N3	118.33428	N9-C5-C4-N3	179.39943
H8-C4	1.12196	N9-C5-C4	121.66378	H10-C6-N1-C2	-179.42800
N9-C5	1.44596	H10-C6-N1	120.00081	H11-C7-C2-N1	0.00736
H10-C6	1.12197	H11-C7-C2	119.99695	H12-C7-C2-N1	-179.42712
H11-C7	1.02801	H12-C7-C2	119.99742	O13-C9-C5-C4	0.63376
H12-C7	1.02788	O13-C9-C5	119.99873	O14-C9-C5-C4	-178.79326
O13-C9	1.13181	O14-C9-C5	119.99998		
O14-C9	1.31592				

[*] for numbering of atom refer Fig. 1

Table 3. Definition of internal coordinates of 2A5NP

No(i)	symbol	Type	Definition
Stretching 1-2	r_i	C-C	C4-C5,C5-C6
3-8	S_i	C-N	N1-C2,C2-N3,N3-C4,C6-N1, C2-N7,C5-N9
9-10	p_i	C-H	C4-H8,C6-H10
11-12	s_i	N-O	N9-O13, N9-O14
13-14	P_i	N-H	N7-H11, N7-H12
Bending 15-20	α_i	N-C-N	N1-C2-N3,C2-N3-C4,N3-C4-C5, C4-C5-C6,C5-C6-N1,C6-N1-C2
21-24	θ_i	N-C-H	N3-C4-H8, C5-C4-H8, C5-C6-H10, N1-C6-H10.
25-26	β_i	N-C-N	N1-C2-N7, N3-C2-N7
27-28	n_i	C-N-O	C5-N9-O13, C5-N9-O14
29	ε_i	O-N-O	O14-N9-O13
30-31	γ_i	C-C-N	C4-C5-N9, C6-C5-N9
32-33	μ_i	C-N-H	C2-N7-H11, C2-N7-H12
34	ν_i	H-N-H	H11-N7-H12
Out-of-plane 35-36	ω_i	C-H	H8-C4-N3-C5, H10-C6-C5-N1
37	ξ_i	C-N-O	C5-N9-O13-O14
38-40	Ω_i	C-N	C2-N7-H11-H12, N7-C2-N1-N3, N9-C5-C4-C6
Torsion 41-46	τ_i	C-C	N1-C2-N3-C4,C2-N3-C4-C5, N3-C4-C5-C6,C4-C5-C6-N1, C5-C6-N1-C2,C6-N1-C2,N3
47	τ_i	N-H	N3(N1)-C2-N7-H11(H12)
48	τ_i	N-O	C4(C6)-C5-N11-O17(O18)

[*] for numbering of atom refer Fig.1

Table 4. Definition of local symmetry coordinates and the value corresponding scale factors used to correct the force fields for 2A5NP

No.(i)	Symbol[a]	Definition[b]	Scale factors used in calculation
1-2	C-C	r1,r2	0.914
3-8	C-N	S3,S4,S5,S6,S7,S8	0.914
9-10	C-H	p9, p10	0.992
11-12	N-O	s11,s12	0.992
13-14	N-H	P13,P14	0.995
14	N-C-N	$(\alpha 15-\alpha 16+\alpha 17-\alpha 18+\alpha 19-\alpha 20)/\sqrt{6}$	0.992
16	N-C-N	$(2\alpha 15-\alpha 16-\alpha 17+2\alpha 18-\alpha 19-\alpha 20)/\sqrt{12}$	0.992
17	N-C-N	$(\alpha 16-\alpha 17+\alpha 19-\alpha 20)/2$	0.992
18-19	N-C-H	$(\theta 21-\theta 22)/\sqrt{2}$,$(\theta 23-\theta 24)/\sqrt{2}$	0.916
20	N-C-N	$(\beta 25-\beta 26)/\sqrt{2}$	0.923
21	C-N-O	$(n27-n28)/\sqrt{2}$	0.923
22	O-N-O	$\varepsilon 29$	0.923
23	C-C-N	$(\gamma 30-\gamma 31)/\sqrt{2}$	0.990
24	C-N-H	$(\mu 32-\mu 33)/\sqrt{2}$	0.990
25	H-N-H	$\nu 34$	0.990

26-27	C-H	ω35,ω36	0.994
28	C-N-O	ξ37	0.994
29-31	C-N	Ω38, Ω39, Ω40	0.962
32	tring	(τ41-τ42+τ43-τ44+τ45-τ46)/√6	0.994
33	tring	(τ41-τ43+τ44-τ46)/2	0.994
34	tring	(-τ41+2τ42-τ43-τ44+2τ45-τ46)/√12	0.994
35	N-H	τ47/4	0.979
36	N-O	τ48/4	0.979

aThese symbols are used for description of the normal modes by TED in Table 5.

bThe internal coordinates used here are defined in Table 3.

Table 5. Detailed assignments of fundamental vibrations of 2A5NP by normal mode analysis based on SQM force field calculation

S. No.	Symmetry species C_s	Observed frequency (cm^{-1})		Calculated frequency (cm^{-1}) with B3LYP/6-311+G ** force field				TED (%) among type of internal coordinates[c]
		Infrared	Raman	Unscaled	Scaled	IR[a] A_i	Raman[b] I_i	
1	A'	3755	3752	3756	3750	67.534	67.877	NH(100)
2	A'	3626		3623	3621	169.095	214.338	NH(100)
3	A'			3230	3228	0.362	87.468	CH(99)
4	A'		3230	3229	3227	0.362	41.679	CH(99)
5	A'	1673		1677	1674	780.767	17.392	CN(46),bHNH(34),bring(10)
6	A'			1650	1648	301.251	6.812	NOas(56),CC(16),bNO2r(11),bCN(7)
7	A'		1655	1649	1647	16.721	36.051	CN(41),bHNH(24),bCH(16),CC(13),bring(5)
8	A'	1578		1585	1582	0.101	2.134	CC(30),NOas(25),CN(24),bCH(7),bring(6)
9	A'	1520	1525	1520	1516	99.739	49.361	CN(47),bHNH(26),bCH(11),bring(10)
10	A'			1460	1458	1.551	0.019	CN(52),bCH(24),CC(7),bCN(7)
11	A'	1414		1415	1410	29.344	56.040	CN(44),bCH(33),NOss(8),CC(6)
12	A'	1396	1386	1395	1391	652.037	269.359	NOss(59),CN(20),bNO2sc(14)
13	A'			1330	1327	14.850	0.449	bCH(68),CN(12),bCNH(12),bNCN(7)
14	A'		1315	1316	1312	0.664	5.041	CN(65),CC(25),bCNH(6)
15	A'	1195		1190	1187	55.705	21.166	CN(33),CC(27),bCH(18),bring(14),NOss(8)
16	A'			1049	1046	0.048	4.054	bring(53),CN(20),CC(19),bCH(7)
17	A'	1034		1046	1043	5.515	1.600	bCNH(56),CN(38)
18	A"		1020	1017	1014	0.001	3.720	gCH(95)
19	A"	982		1005	1003	6.827	3.027	gCH(82),tring(10),gCN(7)
20	A'		888	890	895	1.310	31.481	CN(77),bring(12),CC(6)
21	A'	866		855	850	25.978	4.888	bNO2sc(54),bring(17),CN(13),NOss(11)
22	A"		816	821	818	29.222	0.009	tring(54),gCN(39),gCH(5)
23	A"	745		755	750	5.256	2.099	gCNO(78),gCN(12),gCH(5)
24	A'		682	685	680	13.634	2.123	bring(51),bNO2sc(24),CN(20)
25	A'	661		668	662	5.222	3.750	bring(80),bNCN(7),CC(6)
26	A"			589	585	0.000	2.722	tNH2(98)
27	A'	542	543	541	538	10.096	2.645	bNO2r(54),bCN(19),CC(9),bNCN(8)
28	A"			520	514	0.429	0.001	gCN(53),tring(47)
29	A"			430	426	0.000	0.376	tring(91),gCH(8)
30	A'		415	413	409	10.299	0.140	bNCN(62),bCNH(13),bNO2r(10),bring(9)
31	A'			382	378	0.210	2.420	CN(44),bring(43),bNO2sc(9)
32	A"			275	270	38.671	0.077	gCN(65),tring(28)
33	A'		230	224	220	0.692	1.094	bCN(67),bNO2r(16),bNCN(9)
34	A"			162	159	234.089	0.163	gCNH(79),gCN(18)
35	A"			101	98	2.473	1.322	tring(87),gCNH(6)
36	A"		75	74	70	0.000	0.023	tNO(90),tring(7)

Abbreviations used: b, bending; g, wagging; t, torsion; s, strong; vs, very strong; w, weak; vw, very weak;

[a] Relative absorption intensities normalized with highest peak absorption

[b] Relative Raman intensities calculated by Eq. 1 and normalized to 100.

[c] For the notations used see Table 4.

Table 6. The dipole moment (μ) and first-order hyperpolarizibility (β) of 2A5NP derived from DFT calculations

β_{xxx}	2.9601
β_{xxy}	255.49
β_{xyy}	408.31
β_{yyy}	-2080.9
β_{zxx}	-2.4934
β_{xyz}	-153.82
β_{zyy}	-216.28
β_{xzz}	83.363
β_{yzz}	-12739
β_{zzz}	66.937
β_{total}	4.2557
μ_x	2.24738746
μ_y	0.00038083
μ_z	1.36717199
μ	1.90129963

Dipole moment (μ) in Debye, hyperpolarizibility $\beta(-2\omega;\omega,\omega)$ 10^{-30}esu.

Table 7. Computed absorption wavelength (λ_{ng}) , energy (E_{ng}), oscillator strength (f_n) and its major contribution

N	λ_{ng}	E_{ng}	f_n	Major contribution
1	252.1	4.92	0.0001	H-5->L+0(+41%), H-4->L+0(24%)
2	218.7	5.67	0.0095	H-1->L+1(+61%)
3	214.7	5.78	0.0026	H-4->L+0(+35%), H-1->L+1(25%)

(Assignment; H=HOMO,L=LUMO,L+1=LUMO+1,etc.)

The electric dipoles may enhance, oppose or at least bring the dipoles out of the required net alignment necessary for NLO properties such as β_{total} values. The connection between the electric dipole moments of an organic molecule having donor–acceptor substituent and first hyperpolarizability is widely recognized in the literature [22]. The maximum β was due to the behavior of non-zero μ value. One of the conclusions obtained from this work is that non-zero μ value may enable the finding of a non-zero β value. Of course Hartee–Fock calculations depend on the mathematical method and basis set used for a polyatomic molecule.

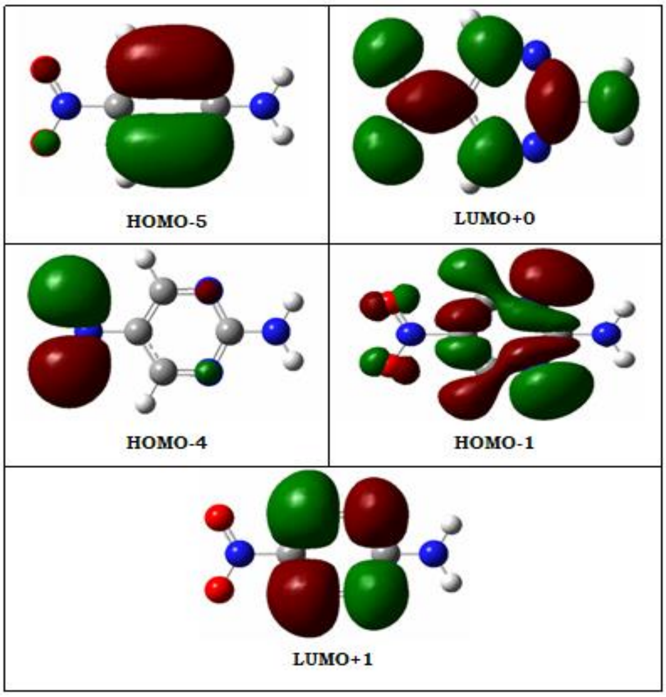

Fig. 5. Representation of the orbital involved in the electronic transition for (a) HOMO-5 (b) LUMO+0 (c) HOMO-4 (e) HOMO-1 (d) LUMO+1

Fig. 4 shows the highest occupied molecule orbital (HOMO) and lowest unoccupied molecule orbital (LUMO) of 2A5NP. There is an inverse relationship between hyperpolarizability and HOMO–LUMO.

HOMO energy = -0.057 a.u
LUMO energy = 0.000 a.u
HOMO–LUMO energy gap = 0.057 a.u

Electronic excitation mechanism

The static polarizability value[23-24] is proportional to the optical intensity and inversely proportional to the cube of transition energy. With this concept, larger oscillator strength (f_n) and $\Delta\mu_{gn}$ with lower transition energy (E_{gn}) is favourable to obtain large first static polarizability values. Electronic excitation energies, oscillator strength and nature of the respective excited states were calculated by the closed-shell singlet calculation method and are summarized in Table 7. Representation of the orbital involved in the electronic transition was shown in Fig. 5.

Conclusions

Complete vibrational analysis of 2A5NP was performed on the basis of DFT calculations at the B3LYP/6-311+G** level. The role of NH_2, NO_2, C-C, C-H and C-N vibrations was discussed in 2A5NP. The various modes of vibrations were unambiguously assigned based on the results of TED output obtained from the normal coordinate analysis. The first-order hyperpolarizibility (β_{ijk}) of the novel molecular system of 2A5NP is calculated using 6-311+G** basis set based on finite field approach. The first-order hyperpolarizibility (β_{total}) of 2A5NP was calculated and found to be 4.2557x10^{-30} esu, which is nearly 22 times greater than that of urea (0.1947 x 10^{-30} esu). Hence these materials have been motivated by their wide range of potential applications such as second harmonic generation (SHG), electro-optic modulation, sum and difference frequency doubling of lasers, etc. Such materials have large nonlinear optical coefficients, suitable transparency and excellent comprehensive properties. Electronic excitation energies, oscillator strength and nature of the respective excited states were calculated by the closed-shell singlet calculation method.

Reference

1. J.G. Contreras, V. Seguel, Spectrochim. Acta 48A (1992) 525.
2. A. Pullman, Pullman, Adv. Hetroeycl. Chem. 13 (1971) 77.
3. J.G. Contreras, S.V. Seguel, Bol. Soc. Chil. Quim. 27 (1982) 5.
4. M. J. Frisch, G. W. Trucks, H. B. Schlegel, G. E. Scuseria, M. A. Robb, J. R. Cheeseman, J. A. Montgomery, Jr., T. Vreven, K. N. Kudin, J. C. Burant, J. M. Millam, S. S. Iyengar, J. Tomasi, V. Barone, B. Mennucci, M. Cossi, G. Scalmani, N. Rega, G. A. Petersson, H. Nakatsuji, M. Hada, M. Ehara, K. Toyota, R. Fukuda, J. Hasegawa, M. Ishida, T. Nakajima, Y. Honda, O. Kitao, H. Nakai, M. Klene, X. Li, J. E. Knox, H. P. Hratchian, J. B. Cross, C. Adamo, J. Jaramillo, R. Gomperts, R. E. Stratmann, O. Yazyev, A. J. Austin, R. Cammi, C. Pomelli, J. W. Ochterski, P. Y. Ayala, K. Morokuma, G. A. Voth, P. Salvador, J. J. Dannenberg, V. G. Zakrzewski, S. Dapprich, A. D. Daniels, M. C. Strain, O. Farkas, D. K. Malick, A. D. Rabuck, K. Raghavachari, J. B. Foresman, J. V. Ortiz, Q. Cui, A. G. Baboul, S. Clifford, J. Cioslowski, B. B. Stefanov, G. Liu, A. Liashenko, P. Piskorz, I. Komaromi, R. L. Martin, D. J. Fox, T. Keith, M. A. Al-Laham, C. Y. Peng, A. Nanayakkara, M. Challacombe, P. M. W. Gill, B. Johnson, W. Chen, M. W. Wong, C. Gonzalez, and J. A. Pople, Gaussian, Inc., Pittsburgh PA, 2003.
5. A.D. Becke, J. Chem. Phys., 98 (1993) 5648.
6. C. Lee, W. Yang, R.G. Parr, Phys. Rev., B37 (1988) 785.
7. G. Foragarasi, P. Pulay, in: J.R. Durig (Ed.), Vibrational Spectra and Structure, vol. 14, Elsevier, Amsterdam, 1985, pp. 125–219.
8. P. Pulay, in: H.F. Schaefer III (Ed.), Application of Electronic structure Theory, Modern Theoretical Chemistry, vol. 4, Plenum press, New York, 1997, p. 153.
9. G. Forgarasi, X. Zhou, P.W. Taylor, P. Pulay, J. Am. Chem. Soc. 114 (1992) 8191.
10. T. Sundius, MOLVIB: a program for harmonic force field calculations. QCPE Program no. 604, J. Mol. Struct. 218 (1990) 321.
11. T. Sundius, Vib. Spectrosc. 29 (2002) 89.
12. G. Keresztury, S. Holly, J. Varga, G. Besenyei, A.Y. Wang, J.R. Durig, Spectrochim. Acta 49A (1993) 2007.
13. G. Keresztury, in: J.M. Chalmers, P.R. Griffiths (Eds.), Raman Spectroscopy: Theory in Handbook of Vibrational Spectroscopy, vol.1, John Wiley & Sons Ltd., 2002.
14. P. Pulay, G. Fogarasi, F. Pong, J.E. Boggs, J. Am. Chem. Soc.,101 (1979) 2550.
15. T. Ziegler, Chem. Rev. 91, 651 (1991).
16. D.N. Sathyanarayana, Vibrational Spectroscopy—Theory and Applications, second ed., New Age International (P) Limited Publishers, New Delhi, 2004.
17. V. Krishna kumar, R. John Xavier, Indian J. Pure Appl. Phys. 41 (2003) 95.
18. G. Socrates, Infrared and Raman Characteristic Group Frequencies, Tables and Charts, third ed., Wiley, Chichester, 2001.
19. B. Wojtkowaik, M. Chabanel, Spectrochimie Moleculaire Technique et Documentation, Paris, 1977.
20. H. Baraistka, A. Labudzinska, J. Terpinski, Laser Raman Spectroscopy: Analytical Applications, PWN-Polish Scientific Publishers/Ellis Harwood Limited Publishers, 1987.
21. D.A. Kleinman, Phys. Rev. 1962;126,1977.
22. P.N. Prasad, D.J. Williams, Introduction to Nonlinear Optical Effects in Molecules and Polymers, Wiley, New York, 1991.
23. K. Wu, C. Liu, C. Mang, Opt. Mater. 29 (2007) 1129–1137.
24. S. Iran, W.M.F. Fabian, Dyes Pigments 70 (2006) 91–96.